

**Size - Strain IV workshop****S - O1****DISLOCATION LINE BROADENING****Radomír Kužel***Department of Electronic Structures, Faculty of Mathematics and Physics,  
Charles University, Prague*

The most complete kinematical theory of X-ray diffraction by real crystals has been formulated by M. A. Krivoglaz [1 – 2]. It allows to classify the lattice defects according to their influence on the diffraction pattern. Theoretical analysis of scattering consisting of the Bragg peak and diffuse lines for different lattice defects and their displacement field shown that the rate of decrease of the displacement field with the distance from the defect determines diffraction effects. The defects with rapidly decreasing field lead to the reduction of integrated intensity (static Debye-Waller factor), shift of the Bragg peaks and appearance of diffuse scattering – these are the so-called defects of the first-kind. The defects with slowly decreasing ( $1/r$ ) displacements destroy the Bragg term and only concentrated diffuse scattering can be observed as the broadened quasiline – the lattice defects of the second kind. Point defects, their clusters, precipitates and small dislocation loops belong to the former while dislocations to the latter type. The type of displacement field plays the most decisive role for the classification of the defects.

This is based on the physical nature of the defects and it has been derived for their random distribution. However, the situation is more complicated in practice. The effects can look differently due to correlation which can screen and reduce the displacement field of the defects in some cases and enhance it under other conditions. Then the defects which belong to the first kind by their physical nature can sometimes look like the 2nd type defects, e.g. because of their high concentration. An interesting case of precipitates and dislocation loops was investigated. Under certain conditions, special doublets of the Bragg and diffuse scattering can be observed simultaneously.

In many cases, the relations for line shift and broadening are given by the product of several functions – function of the diffraction vector, function of the defect strength and the so-called orientation factor which determines the  $hkl$ -dependence of the diffraction parameter and is determined by the orientation of the defects with respect to the diffraction vector and crystallographic axes.

Dislocations and 2nd kind stresses are the main reasons for the so-called strain broadening. The problem was treated by Williamson and Smallman in 1956 [3] but only for a single dislocation. Krivoglaz and Ryaboshapka [4] assumed statistically random distribution of dislocations and derived relations for integral breadth and Fourier coefficients. Integral breadth is proportional to the square-root of dislocation density and the so-called orientation factor determining the  $hkl$ -dependence. Wilkens shown that completely random distribution of dislocations is unrealis-

tic [5] and introduced the so-called restrictedly random distribution characterized by the dislocation density and cut-off radius  $R_c$  (the radius of the region within which the distribution is random). This parameter can be taken as a measure of correlation in dislocation distribution. Krivoglaz, Martynenko and Ryaboshapka [6] generalized their original model by including pair correlation functions and came to similar results. Further extension was done by Ungar, Groma et al. [7] who introduced more parameters and included the case of dislocation polarization. Calculations for dislocation dipoles, dislocation loops and dislocation walls were also performed mostly by Krivoglaz, Ryaboshapka and Barabash [review in 8 and 9, 10]. In recent years, the most frequently used formalism for description of dislocation-induced line broadening is that of Wilkens. However, similar but not identical Krivoglaz description [6] for not too strong correlation in dislocation arrangement can be used as well. It was applied first in [11].

Integral breadth (in  $1/d$ ) can be approximated as follows

$$\frac{1}{d} \approx b \sqrt{\rho} \sqrt{\frac{P}{2A}} \frac{\sin}{hkl} \quad (1)$$

where  $\rho$  is the mean dislocation density,  $b$  is the magnitude of the Burgers vector, the  $P$  factor is related to the correlation in dislocation arrangement and factor  $A$  is close to unity. For dislocation density determination the knowledge of the orientation factor (often called as contrast factor and denoted by  $C$ ) is necessary. The correlation factor  $P$  must be estimated for example from the profile shape or better from Fourier coefficients. The orientation factor depends on the indices  $h, k, l$  and determines the anisotropy of line broadening. The corresponding relations for the most common dislocations in cubic materials were published by Krivoglaz [1]. General relations for calculation of the orientation factors were derived in papers [12, 13] based on the formalism for description dislocation displacement field by Teodosiu and Steeds. In order to calculate the factor, some model – dislocation types must be considered. As each type gives characteristic anisotropy of line broadening, in some cases it is possible to estimate dominating dislocation types from such an anisotropy. Crystal symmetry must be taken into account and corresponding averaging over all symmetrically equivalent directions must be performed for the calculations of orientation factors. The calculations must be numerical in general case of elastic anisotropy. In case of preferred orientation of lattice defects in the sample, appropriate weights must be taken in averaging. If more slip systems are active (and dislocations



with different Burgers vector) it is better to include the Burgers vector in the orientation factor. Useful simple relations for orientation factors of polycrystalline cubic and hexagonal materials without preferred grain and defect orientation were derived by Ungár et al [14 - 16]. Calculations of the orientation factors for non-random defect distribution in thin films were published by Armstrong et al [17, 18].

The correlation factor can be expressed as

$$P = r_c \sqrt{B_{hkl}} \sqrt{R_c} \quad (2)$$

where

$$B_{hkl} = 2 \sum_{i=1}^N b_i^2 \sin^2 \frac{\alpha_i}{2} \quad (3)$$

for the case of more dislocation slip systems. The quantity  $R_c$  is the cut-off radius and  $r_c$  is its value modified by the second orientation factor  $r_c$ . In general, the calculation of  $P$  is more complicated. It depends itself on the dislocation density and the value  $r_c$  is unknown. Its value can be estimated from the profile shape. We can take rough estimation as follows: for  $P = 3$  is the shape between Cauchy and quadratic Cauchy (C2) functions,  $P = 5$  corresponds to C2, for higher  $P$  it is close to the Gauss function. Hence, with the increasing correlation in dislocation arrangements the profile tails are extended. For the estimation also the dependence of ratio FWHM/ vs.  $P$  can also be used. However, the profile shape is sensitive to  $P$  only for small  $P$  values. On the other hand, the dependence vs.  $\sin$  is justified strictly speaking only for  $P > 3$  [6].

For precise evaluation, the Fourier analysis, must be applied

$$\ln A_h(L) = B_h L^2 \ln \frac{r_c}{L} \quad (4)$$

It follows that the plot  $\ln A(L)/L^2$  vs.  $\ln L$  should be linear (at least in the region of validity of the used approximations, i.e. medium values of  $L$ ). The slope of the plot then gives  $B_{hkl}$  and the  $\ln L$  intercept the value  $\ln r_c$ , i.e. also the correlation factor  $P$ . Instead of the simple but diverging logarithmic term two functions were suggested by Wilkens and van Berkum. This formalism is used for the description of dislocation line broadening in two programs using the method of total powder pattern fitting (or multiple profile fitting) – program by Leoni and Scardi [19], and Ribarik and Ungár [20, 21] (see more in their lectures at this conference and also on the posters). Usually the  $hkl$  dependence of  $r_c$  is neglected. However, in principle it can also be assumed [lecture of Armstrong at this workshop].

Quite detailed analysis of inhomogeneous distribution of dislocations is possible from careful measurements of profile tails and evaluation of moments [22, see also the lecture of Borbély at this workshop].

In spite of the fact the line profile analysis of dislocation-induced line broadening has been improved in last years, there are still problems bigger than in crystallite size description. This is especially high correlation between dislocation density and dislocation-correlation factor which makes the fitting difficult. The latter determines the shape of the profile however, careful measurement with high statistics of counts is necessary in order to use this fact. The correlation is inherent in the description and can-

not be completely overcome by different optimization algorithms. While for nearly random distribution of dislocations the methods work well, for highly-correlated or strongly inhomogeneous distribution of dislocations appropriate description which could be easily applied in the profile analysis is missing.

Nearly no studies were devoted to relations and/or separation between the broadening caused by the 2nd kind stresses and by dislocations. The only attempt was published in [23].

- [1] M.A. Krivoglaz, Theory of X-ray and Thermal Neutron Scattering by Real Crystals, Plenum Press, New York 1969.
- [2] M.A. Krivoglaz, X-ray and Neutron Diffraction in Nonideal Crystals, Springer-Verlag, Berlin 1996.
- [3] G. K. Williamson and R.E. Smallman, Philos.Mag. **1**, 34-46 (1955).
- [4] M.A. Krivoglaz and K.P. Ryaboshapka, Phys.Met.Metallogr. **15**, 14(1963).
- [5] M. Wilkens, Phys.Stat.Sol. **A2**, 359(1970).
- [6] M.A. Krivoglaz, O.V. Martynenko and K.P. Ryaboshapka, Fiz.Met.Metalloved **55**, 5-17 (1983).
- [7] T. Ungár, I. Groma and M. Wilkens, J.Appl.Cryst. **22**, 26(1989).
- [8] R.I. Barabash, In *Defect and Microstructure Analysis by Diffraction*. (Eds. R.L. Snyder, J. Fiala and H.J. Bunge) pp. 127-140, Oxford University Press, Oxford 1999.
- [9] In *Advances in Structure Analysis*, Czech and Slovak Crystallographic Association, Prague, 2001 (eds. R. Kužel, J. Hašek). Paper by R. I. Barabash, P. Klimanek. 438 – 448.
- [10] R. I. Barabash, P. Klimanek, *J. Appl. Cryst.* (1999). **32**, 1050-1059
- [11] R. Kužel and P. Klimanek, *J.Appl.Cryst.* **22**, 299-307 (1989).
- [12] P. Klimanek and R. Kužel, *J.Appl.Cryst.* **21**, 59-66 (1988).
- [13] P. Klimanek and R. Kužel, *J.Appl.Cryst.* **21**, 363-68 (1988).
- [14] T. Ungár and G. Tichý, *Phys.Stat.Sol.* **17**, 42-43 (1999).
- [15] T. Ungár, I. Dragomir, A. Révész and A. Borbély, *J.Appl.Cryst.* **32**, 992-1002 (1999).
- [16] I. Dragomir, T. Ungár, *J. Appl. Cryst.* (2002). **35**, 556-564.
- [17] R. Cheary, E. Dooryhee, P. Lynch, N. Armstrong, S. Dligatch, *J. Appl. Cryst.* (2000). **33**, 1271-1283
- [18] in *Diffraction Analysis of the Microstructure of Materials* (ed. E. J. Mittemeijer, P. Scardi), Springer, Berlin, 2004, chp. Armstrong, Lynch, p.249 -286.
- [19] P. Scardi, M. Leoni, *Acta Cryst.* **A58**, 190-200 (2002).
- [20] G. Ribárik, T. Ungár and J. Gubicza, *J.Appl.Cryst.* **34**, 669-676 (2001).
- [21] T. Ungár, J. Gubicza, G. Ribárik and A. Borbély, *J.Appl.Cryst.* **34**, 298-310 (2001).
- [22] in *Diffraction Analysis of the Microstructure of Materials* (ed. E. J. Mittemeijer, P. Scardi), Springer, Berlin, 2004, chp. Groma, Borbély, p.287 - 307.
- [23] D. Breuer, P. Klimanek, W. Pantleon *Appl. Cryst.* (2000). **33**, 1284-1294.



S - O2

**DISCLINATIONS AND REAL STRUCTURE OF MATERIALS****P. Klimanek***Institute of Physical Metallurgy, TU Bergakademie Freiberg, Gustav-Zeuner-Str. 5, D-09599 Freiberg, Germany*

S - O3

**STACKING DISORDER AND ITS ANALYSIS BY X-RAY DIFFRACTION****Ernesto Estevez-Rams, Cristy Azanza-Ricardo, Beatriz Aragon-Fernandez\*, Arbelio Penton-Madrigal***Instituto de Materiales y Reactivos. Universidad de la Habana. San Lazaro y L. CP 10400, C. Habana, Cuba  
\*Centro de Investigaciones Metalurgicas, Calle 51 esq a 240, La Lisa, C. Habana, Cuba*

The study of planar faulting by X-ray diffraction has a long history dating from the first works in diffractions. (Early contributions have been reviewed in [1], while further developments can be found in [2]).

Two types of methods have been so far used, (1) those which derive a set of useful parameters related to some assumed faulting model and (2) those based on computer simulations and Monte Carlo procedures which match simulated patterns with the experimental ones.

There are several limitations to both approaches. In the first type, Warren's use of difference equations [1, 3] is the most used: peak shift, broadening and asymmetry are related to the probabilities of deformation and twin faulting. As pointed out recently [4], the original approach can lead to wrong predictions of the faulting effects on diffraction profiles. Another drawback is the lack of generality, the methods need of specific derivations for different structures and faulting types.

Concerning Monte Carlo schemes, these are trial and error procedures matching simulated patterns with experimental ones. Simulation procedures are better suited than Warren's approach for investigating complex faulted structures. Yet, simulations strongly rely on the ability of the researchers to propose faulting models suitable to the investigated problem, and they make little use of the observed experimental data until the last stages of analysis, where comparison is performed.

A recent approach by the authors derives quantitative information about the stacking order in layer crystals directly from diffraction data, without assuming any prior model for the stacking disorder [5, 6]. The original formulation was valid for powder diffraction data with one type of layer in the stacking sequence and a integer number of times a constant displacement vector between the different possible layer positions. The solution of the diffraction equations allowed, in a general framework, to derive features of powder diffraction patterns of faulted layer crystals and better understand the effect of faulting in the diffraction pattern [6, 7]. The relation between the symmetric and asymmetric component of broaden peaks were explored for the general close packed case [7]. This allowed avoiding

the arbitrariness in the modeling of peak profiles affected by faulting.

In this presentation we will review the latest work done by the authors in the analysis of diffraction pattern of samples with planar disorder. Some theoretical developments will be reviewed together with applications to real data will be shown.

If we lift the restriction on the same type of layer for the diffraction equations the expression for the interference functions (definitions and more detailed mathematical background can be found in [4, 5]) can be written as:

$$Q(r^*) = 2 \sum_{0 \leq w \leq N_3} \text{Re} F_w(r^*) F_w^*(r^*) \cos[2(R_w - R_w)] + \sum_{0 \leq w \leq N_3} \text{Im} F_w(r^*) F_w^*(r^*) \sin[2(R_w - R_w)] \quad (1)$$

Expression (1) reduces to the ones already derived in [4] for structures with all layers having the same structure factor:

$$Q(r^*) = 2 |F(r^*)|^2 \sum_{0 \leq w \leq N_3} \cos[2(R_w - R_w)] \quad (2)$$

In the case of a constant structure factor per layer, the interference function (experimental observable) can be related to the probability correlation function which describes the stacking ordering of the layers [5, 6]. The problem of the diffraction pattern of planar disordered structures then reduces to the extraction from the available data of the probability correlation function.

It has been shown in [7] that (2) forces a relation between the symmetric and asymmetric component of the peak broadening. This biunivocal relation implies that once a symmetrical component is chosen the asymmetrical component is completely determined, which reduces, at least in this sense, the arbitrariness of the asymmetry modeling. The relations can also be used to address the implications of an assumed peak profile model in the underlying planar disorder.



Table 1

Profile	Symmetric term	Asymmetric term
Gaussian	$G^s(r^*) = \frac{2}{f} \sqrt{\frac{\log 2}{\pi}} \exp\left(-4 \log 2 \left(\frac{l-l_0}{f}\right)^2\right)$	$G^A(r^*) = \frac{1}{2} \exp\left(-\frac{l-l_0}{c}\right) \sin[2(l-l_0)]$
Lorentzian	$L^s(r^*) = \frac{1}{2f} \frac{1}{1 + 2\left(\frac{l-l_0}{f}\right)^2}$	$L^A(r^*) = \frac{2(l-l_0)}{\cosh\left(\frac{l-l_0}{c}\right) + 1 + 2\left(\frac{l-l_0}{f}\right)^2}$
Pseudo Voigt	$pV^s(r^*) = G^s(r^*) + (1-\eta)L^s(r^*)$	$pV^A(r^*) = G^s(r^*) + (1-\eta)L^A(r^*)$
Pearson VII	$pVII^s(r^*) = i_0 \frac{1}{1 + 2\sqrt{m}(2^{1/m}-1)\left(\frac{l-l_0}{f}\right)^{2/m}}$	$pVII^A(r^*) = \frac{1}{2} \sqrt{\frac{f}{0}} K_{m-1/2} \frac{f}{0} \sin[2(l-l_0)]$

Table 1 shows the corresponding expression of the asymmetric component for common used symmetrical profiles:

#### Acknowledgement

EER will like to thank the Alexander von Humboldt Foundation for the sustained support. This work was partially done under an Alma Mater grant.

[1] Welberry, T. R., 1985, Rep. Prog. Phys., 48, 1543.

[2] Ustinov, A. I., 1994, Defect and Microstructure Analysis by Diffraction, edited by R. L. Snyder, J. Fiala and H. J.

Bunge (Oxford: Oxford Science Publications), chapter 15, pp. 264–316.

[3] Warren, B. E., 1990, X-ray Diffraction (New York: Dover Publications).

[4] Velterop, L., Delhez, R., Keijsers, Th. H., Mittemeijer, E. J., and Reefman, D., 2000, J. Appl. Crystallogr., 33, 296.

[5] Estevez-Rams, E., Martinez, J., Penton-Madrigal, A., and Lora-Serrano, R., 2001, Phys. Rev. B, 63, 54 109.

[6] E. Estevez-Rams, I. B. Aragon-Fernandez, H. Fuess, and A. Penton-Madrigal, 2003, Phys. Rev. B, 68, 064111.

[7] E. Estevez-Rams, M. Leoni, P. Scardi, B. Aragon-Fernandez, Phil. Mag., 83 (2003) 4045.SS4-O4

S - O4

## SOME CONSIDERATIONS CONCERNING WILKENS' THEORY OF DISLOCATION LINE-BROADENING

N. Armstrong<sup>1</sup>, M. Leoni<sup>2</sup> & P. Scardi<sup>2</sup>

<sup>1</sup>Department of Applied Physics, University of Technology Sydney, PO Box 123, Broadway, NSW 2007, Australia

<sup>2</sup>Dipartimento di Ingegneria dei Materiali e Tecnologie Industriali, Università di Trento, 38050 Trento, Italy.

X-ray line profile analysis is a potentially powerful non-destructive method for characterising the microstructure of materials. In the past decade, the technique has quickly evolved from a stage where “simple” assumptions were made concerning the shape and breadth of line profiles to state-of-art methods, allowing the synthesis of diffraction profiles directly from the microstructural properties of materials (see [1] for state-of-art methods). These microstructural properties include, lattice faulting/twinning, dislocations and crystallite shape and size distributions (see [1] and reference therein).

However, not all available models have reached their maturity. In particular, the Wilkens model [2-4] is commonly adopted for the (Fourier) description of X-ray line-profile broadening caused by the presence of dislocations. In this contribution, some insights concerning its physical significance and interpretation will be presented.

The Wilkens model provides analytical expressions for the Fourier transform of a line profile broadened by dislo-

cations in terms of two free parameters: the average dislocation density and the effective outer cut-off radius  $R_c$  of the strain field. This model was developed assuming a simple microstructure in which a restrictedly random distribution of dislocations is present. This means that equal numbers of parallel and antiparallel straight dislocations populate a single slip-system and are randomly distributed within a sub-area  $F_p$  of the total area  $F_0$  [2]. A number of important assumptions are made in this case: (i) the radius  $R_p$  of the sub-area is approximately equal to the outer cut-off radius  $R_c$ ; (ii) the total dislocation density is uniform i.e. the ratio between the total number of dislocations  $N_0$  and the total cross-sectional area  $F_0$  and the ratio between the number  $N_p$  of dislocations in the sub-area and the area of such region  $F_p$  are equal:  $N_0/F_0 = N_p/F_p$ . These assumptions are necessary to overcome the logarithmic divergence encountered by Krivogolaz & Ryaboshapka [5] in

their alternative formulation of dislocation broadened line profiles.

It will be shown here that two formulations of the Wilkens model can be developed (see [2, 3]); diffraction patterns for (real) elastically anisotropic materials will be simulated, showing qualitative and quantitative differences in the result of the two models.

The first and most widely used formulation [1] will be termed *simplified Wilkens model*. It assumes that the “average” Fourier term is independent of the slip system, the only *hkl* dependence being carried by the average contrast factor  $\langle C_{hkl} \rangle$  and by the reciprocal interplanar distance  $d_{hkl}^*$  [2, 3].

The second formulation, called *full Wilkens model*, includes the slip-system and *hkl* dependencies into the Fourier coefficients, therefore expressing the resultant Fourier coefficients as the convolution product:

$$A(L, d_{hkl}^*) = \prod_{j=1}^N A_j(L, d_{hkl}^*) \exp \left[ -\frac{b^2 (d_{hkl}^*)^2 L^2}{2} \frac{1}{N} \prod_{j=1}^N C_{hkl}^j f^*(j) \right] \quad (1)$$

where  $A_j(L, d_{hkl}^*)$  is the Fourier transform for the *j*-th slip-system, *b* is the magnitude of Burgers vector, *L* is the Fourier length,  $\frac{1}{N} \prod_{j=1}^N C_{hkl}^j f^*(j)$  defines the slip-depend-

ency of the contrast factors and is Wilkens function (see [2]).

A set of simulated patterns for Cu, Ni and CeO<sub>2</sub> will be employed to highlight the difference between the two models. Simulations are made assuming an ideal diffractometer with CuK wavelength, dislocations density,  $\times 10^{16} \text{ m}^{-2}$  and an effective outer cut-off radius,  $R_c = 10.0 \text{ nm}$ . These setting correspond to a Wilkens parameter  $M = R_c^{1/2} = 1.4$ , which is within the range of applicability of the theory [2-4]. These simulations highlight the slip-system and *hkl* dependency of the quantities in (1) and the influence they have on the profile for increasing  $d_{hkl}^*$ .

- [1] E. J. Mittemeijer & P. Scardi, editors: *Diffraction Analysis of the Microstructure of Materials*, Springer Series in Materials Science, Vol. 68. (Springer-Verlag, Berlin, 2004).
- [2] M. Wilkens (1970a), *NBS Spec. Publ. 317*, **2**, 1195–1221. Proceedings of *Fundamental aspects of dislocation theory*, eds. J. A. Simmons, R. De Witt and R. Bullough.
- [3] M. Wilkens (1970b), *NBS Spec. Publ. 317*, **2**, 1191–1193. Proceedings of *Fundamental aspects of dislocation theory*, eds. J. A. Simmons, R. De Witt and R. Bullough.
- [4] M. Wilkens (1970c), *Phys. Stat. Sol. A*, **2**, 359–370.
- [5] A. Krivoglaz & K. P. Ryaboshapka, *Fiz. Metal. Metalloved.*, 15(1), 18–31.

S - O5

## STATUS OF NIST NANOCRYSTALLITE SIZE SRM 1979

N. Armstrong<sup>1</sup>, J. P. Cline<sup>2</sup>, W. Kalceff<sup>1</sup>, J. Ritter<sup>2</sup> & J. Bonevich<sup>3</sup>

<sup>1</sup>Department of Applied Physics, University of Technology Sydney, AUSTRALIA

<sup>2</sup>Ceramics & <sup>3</sup>Metallurgy Divisions, National Institute of Standards and Technology (NIST), USA.

The NIST nanocrystallite size Standard Reference Material (SRM) 1979 will provide a standard for both scientific and commercial laboratories to quantify the size distribution and shape of nanocrystallites using X-ray line profile and electron microscopy techniques. It will also apply a Bayesian/Maximum entropy (MaxEnt) method of X-ray diffraction data analysis especially developed for certifying the SRM. It is expected that SRM 1979 will play a pivotal role in the rapidly developing nanotechnology industry by providing uniformity in the measurement of crystallite size and shape data, while clarifying the underlying assumptions of many existing line profile techniques.

In this paper we discuss the preparation and analysis of the two proposed SRM 1979 candidate materials. An outline of the procedure is given, together with a detailed discussion of the X-ray line profile analysis used to determine both the size and shape information of the SRM 1979 specimens.

SRM 1979 will consist of two material specimens prepared in 1kg batches from bulk feedstock. The specimens have been produced to minimize the presence of structural defects that may result in strain broadening in the line profiles. The first material sample is ceria (cerium (IV) oxide,

CeO<sub>2</sub>) with an (approximate) average spherical crystallite size of 20 nm over a size range of 5–35 nm. The SRM is produced from a precipitation reaction between cerium (IV) sulfate solution and an ammonium hydroxide solution, conducted in a fixed-element flow reactor. Ceria has a cubic symmetry resulting in well-spaced diffraction lines. This allows rapid and simplified analysis techniques to be used to determine the shape and dimensions of the crystallites, while minimizing systematic error arising from overlapping peaks. Moreover, the spherical morphology ensures that the size broadening will be isotropic in *hkl*. This enables models for simple shapes to be applied.

The second SRM 1979 specimen is zinc oxide (ZnO) which is also prepared in a fixed-element flow reactor, by a precipitation reaction between zinc acetate and an ammonium hydroxide solution. This SRM specimen has a cylindrical crystallite morphology with an approximate length of 80 nm and a size range of 60–100 nm. ZnO has a hexagonal symmetry, producing a large number of (overlapped) lines. Consequently, this specimen requires more complex size and shape models to be applied in order to extract the necessary information from the X-ray diffraction data. Specifically, the anisotropic broadening for various *hkl*



provides a direct indication of the crystallite morphology, while the size distribution reveals the spread in the cylinder heights and diameters.

The analysis technique essentially involves two steps [1, 2]. The first step applies MaxEnt/Fuzzy pixel deconvolution methods simply to remove the instrumental broadening, and produce the specimen profile. Using this data, simple microstructural models for the crystallite size/shape (and if necessary defect content) can be developed. This data serves as the *a priori* information for the full Bayesian/MaxEnt analysis constituting the second step. Moreover, this approach provides a basis for developing a series of models from which the most probable model can be determined using Bayesian model selection theory. This analysis takes full account of the form of the instrumental, background and statistical noise contributions embedded in the diffraction data. As well as providing the most probable solution, the second step also produces a full

error analysis of the size distribution—a critical element in certifying SRM 1979.

The X-ray analysis presented here will be compared with the results of direct observations of SRM 1979 using TEM imaging, and a discussion based on this comparison will be presented.

- [1] N. Armstrong, W. Kalceff, J. P. Cline and J. Bonevich (2004), “Bayesian inference of nanoparticle-broadened line profiles”, *J. Res. NIST*. Accepted for publication 11 April 2003.
- [2] N. Armstrong, W. Kalceff, J. P. Cline and J. Bonevich (2003), “A Bayesian/maximum entropy method for certification of a nanocrystalline-size NIST Standard Reference Material”, in Chapter 8, *Diffraction Analysis of the Microstructure of Materials* (eds. E. J. Mittemeijer & P. Scardi), Springer, Berlin, pp.187–227.

S - O6

## WHOLE POWDER PATTERN MODELLING FOR THE STUDY OF NANOCRYSTALLINE AND IMPERFECT MATERIALS

Paolo Scardi & Matteo Leoni

*Department of Materials Engineering and Industrial Technologies, University of Trento, 38050 via Mesiano 77, Trento ITALY, e-mail: Paolo.Scardi@unitn.it*

The growing interest in nanostructured materials and devices has given new impetus to the research on diffraction Line Profile Analysis (LPA). Concurrently, the research on powder diffraction techniques moved toward an increasing integration of methods, in the attempt at providing structural and microstructural information from a single, combined refinement procedure.

The *Whole Powder Pattern Modelling (WPPM)* approach was devised according to the philosophy of analysing powder diffraction data on the base of physical models of the real microstructure, without using a priori fixed analytical peak-profile functions. Main models consider the effect of (i) crystalline grain shape and size distribution, (ii)

line defects (dislocations), (iii) structural mistakes (e.g., planar defects like twin and deformation faults or anti-phase domain boundaries) and (iv) grain surface-relaxation effects, but in principle any possible source of line profile effects can be easily included in the general WPPM algorithm.

The present work addresses recent developments in the WPPM approach. Besides reviewing the basic theory underlying the WPPM, refinement results for nanocrystalline and heavily deformed materials are shown and discussed in comparison with the outcome of traditional line profile analysis methods. Actual limits and future prospects in LPA are also discussed.

S - O7

## COHERENCE OF NANOCRYSTALLINE PARTICLES TO X-RAYS

David Rafaja<sup>1</sup>, Volker Klemm<sup>1</sup>, Gerhard Schreiber<sup>1</sup>, Michael Knapp<sup>2</sup> and Michal Šíma<sup>3</sup>

<sup>1</sup>*Institute of Physical Metallurgy, TU Bergakademie Freiberg, Gustav-Zeuner-Str. 5, D-09599 Freiberg, Germany*

<sup>2</sup>*Institute of Materials Science, TU Darmstadt, Petersenstr. 23, D-64287 Darmstadt, Germany*

<sup>3</sup>*SHM, Nový Malín 266, CZ – 788 03 Nový Malín, Czech Republic*

In the kinematical diffraction theory, individual crystallites are defined as coherent domains and their coherence to X-rays is neglected. This assumption is certainly correct for large crystallites (larger than some tens of nanometers), which are represented by narrow points in the reciprocal space. On the contrary, this assumption may be incorrect in nanocrystalline materials (smaller than 10 nm) with broad

and overlapping reciprocal space points, where a partial coherence of the adjacent crystallites can be anticipated. In X-ray diffraction (XRD) experiments, partly coherent crystallites seem larger because they cannot be distinguished from each other. The partial coherence combined with a slightly different orientation and with a shift of adjacent crystallites causes an additional diffraction line broad-



ening, which is increasing with increasing size of the diffraction vector. Such a diffraction line broadening is then misleadingly interpreted as microstrain. The above phenomena were described theoretically considering that the overlap of the reciprocal space points from adjacent crystallites can serve as a measure of their coherence in the direct space. It was shown that the degree of coherence of the nanocrystalline particles depends on their size as well as on their mutual orientation. The experimental evidence of the coherence of the nanocrystalline particles to X-rays was provided by the comparison of the crystallite size obtained from XRD and from the transmission electron microscopy with high resolution (HRTEM). The

experimental results were obtained on the  $Ti_{1-x}Al_xN$  thin films with different chemical and phase compositions, which were deposited by the arc sputtering from two targets (Ti and Al) in working atmosphere containing nitrogen. In these samples, HRTEM yielded the crystallite size of 35 – 50 Å; the crystallite size obtained from XRD was 35 – 200 Å depending on the degree of coherence of the neighbouring crystallites. The coherence of the adjacent crystallites varied with the degree of the preferred orientation of crystallites and with the phase composition of the samples (cubic ternary solid solution (Ti,Al)N and hexagonal AlN).

**S - O8**

## ANALYTICAL EXPRESSION FOR DIFFRACTION LINE PROFILE FOR POLYDISPERSIVE POWDERS. NEW METHODS FOR GRAIN SIZE DISTRIBUTION DETERMINATION

**Roman Pielaszek, Wittek Lojkowski**

*High Pressure Research Center, Polish Academy of Sciences*

An analytical expression for the diffraction line profile for polydispersive powders (particularly, nanopowders) with Gamma Grain Size Distribution is derived. The expression consists of elementary functions only and can readily replace standard functions (like Gaussian, Lorentzian or Pearson) for diffraction peak fitting purposes. This allows for direct Grain Size Distribution determination using standard fitting software. Well established Scherrer method allows for determination of the average grain size of a crystalline powder by measurement of Full Width at Half Maximum (FWHM) of the diffraction peak profile. Basing on the expression derived, we propose an enhancement of this classical method. Measurement of two

widths of the same peak, allows for two parameters to be distinguished: the average grain size and dispersion of sizes (sigma). These parameters are sufficient to draw Grain Size Distribution (GSD) curve, that is much more informative than a single size parameter.

We propose to measure widths at 1/5 and 4/5 of the peak maximum (FW1/5M and FW4/5M, respectively). A simple algebraic formula that converts measured FW1/5M and FW4/5M values into and (sigma) is presented. The FW1/4/5M method proposed in this paper is especially sensitive in case of a broad diffraction maxima, i.e. for nano-sized polycrystals.

**S - O9**

## TEST OF APPLICABILITY OF SOME POWDER DIFFRACTION TOOLS TO NANOCRYSTALS

**Z. Kaszukur**

*Institute of Physical Chemistry PAS, Warszawa, 01-224 Poland*

Most of the diffraction structure analysis methods developed for polycrystals meet their application limit when crystal size decreases below few nanometers. Measurable effects of nanocrystallinity on the analysis can be noticed already for 10 nm crystallites. The Bragg law itself ceases to apply strictly [1] what appears to be a direct consequence of short atom rows and thus of short, truncated Fourier series in the peak harmonic representation. The surface relaxation effect adds only a minor term to the lattice constant calculated directly from a single peak position. With advent of nanotechnologies and rising interest in experimental analysis of nano-sized structures it is increasingly important to test application limits of the available structural methods.

The structural methods affected include the full profile analysis, methods of separation of size and strain (the Williamson-Hall plot as well as the Warren-Averbach method), methods of a lattice constant determination, quantitative analysis (linearity of the peak intensity – number of atoms dependence) etc.

The tests were performed on the model nanocrystals having distribution of sizes following the log-normal distribution of a crystallite volume. The maximum was centred ~5nm and the model crystallites were cubooctahedral, closed shell fcc structures having from 561 to 24739 atoms. The structure was chosen to be that of palladium metal and the interatomic potentials used for its relaxation followed the Sutton-Chen N-body scheme [2]. Both non-relaxed and

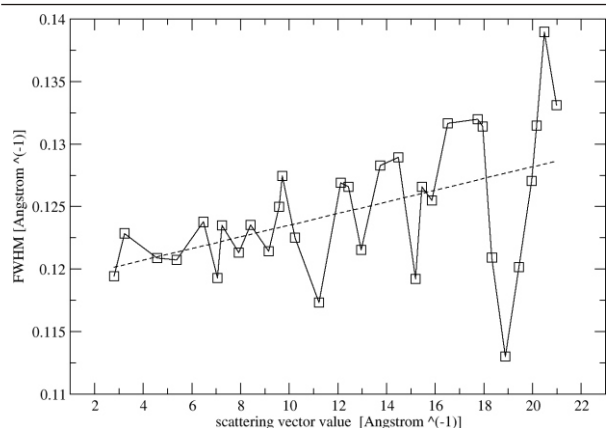


Fig. 1.

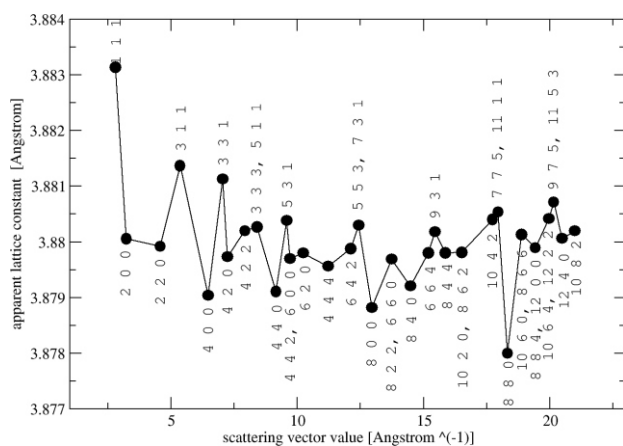


Fig. 2.

energy relaxed models were used to estimate the effects of relaxation.

The diffraction patterns for the model were calculated following the Debye's formula. The patterns were analysed using PEAKFIT program [3] via decomposing the profiles

onto constituent Pearson VII peaks. Due to lack of unequivocal background definition the peak fit parameters may be obtained with some error – this however affects the results only for strongly overlapping peaks. Such peaks were excluded from the data presented in figs. 1,2. Fig.1 shows the apparent lattice constant as obtained from the consecutive peaks position using the Bragg law. It is remarkable that the peaks with the odd Miller indices give the lattice constant value systematically greater than that produced by the even indices. The Williamson-Hall plot (figure 2) displays crystallite size close to the real one and evidently not vanishing stress parameter for the relaxed system pattern.

The Warren-Averbach analysis for the same pattern (002 peak family) enables reconstruction of the original column-length distribution and confirms the presence of a not vanishing stress distribution for the relaxed model. For the models of bimodal log-normal distribution the same analysis fails however in reconstructing the column length distribution in both: maxima positions and their amplitude ratio [4].

The discussed effects are not negligible in a full profile analysis of nanocrystals and are more significant the greater stress is induced to the nanocrystal structure.

#### Acknowledgement

This study was supported by the State Committee for Scientific Research (KBN) grant no. 4T09A 180 24.

- [1] Z. Kaszukur, *J. Appl. Crystallogr.*, **33** (2000) 87.
- [2] A. P. Sutton and J.Chen, *Philos.Mag.Lett.*, **61**, 139 (1990).
- [3] Jandel Scientific GmbH , PEAKFIT (1990), v.3.11, D-40699 Erkrath, Germany.
- [4] Z. Kaszukur, B.Mierzwa, to be published.

S - O10

## MICROSTRUCTURE OF SEVERELY DEFORMED METALS FROM X-RAY PEAK PROFILE ANALYSIS

J. Gubicza<sup>a</sup>, N. H. Nam<sup>a</sup> and V. V. Stolyarov<sup>b</sup>

<sup>a</sup>Department of Solid State Physics, Eötvös University, Budapest, Hungary

<sup>b</sup>Institute of Physics of Perspective Materials, Ufa State Aviation Technical University, Ufa, Russia

E-mail: gubicza@ludens.elte.hu

Severe plastic deformation (SPD) is an effective tool for producing bulk ultrafine grained (submicron grain sized or nanostructured) metals. One of the most common SPD methods is equal channel angular pressing (ECAP) – a technique that results in a homogeneous sub-micron grain structure of the workpiece [1]. The ultrafine grained materials produced by ECAP have an attractive combination of high strength and good ductility due to their low contamination and unique structures. For understanding the mechanical behavior of materials produced by ECAP, it is necessary to characterize their microstructure. In this work the microstructure of cubic TiNi and hexagonal Mg(Al) al-

loy produced by ECAP is studied by X-ray diffraction peak profile analysis. The high resolution X-ray diffraction experiments are performed using a special double-crystal diffractometer (Nonius FR591) with rotating Cu anode [2]. The peak profiles are evaluated by the Multiple Whole Profile (MWP) fitting procedure described in detail in Ref. [3]. In this method, the Fourier coefficients of the experimental profiles are fitted by the theoretical Fourier transforms calculated on the basis of a model of the microstructure [3]. The crystallite size distribution and some characteristic parameters of the dislocation structure (e.g. density and arrangement of dislocations) are obtained from the fitting.



Additionally, the procedure enables the determination of the prevailing dislocation slip systems in the sample [4]. The eleven dislocation slip systems in a hexagonal Mg alloy can be classified into three groups based on their Burgers vectors:  $\langle a \rangle$  type,  $\langle c \rangle$  type and  $\langle c+a \rangle$  type [5]. X-ray diffraction peak profile analysis reveals the abundance of  $\langle a \rangle$ -type dislocations besides the  $\langle c \rangle$ - and  $\langle c+a \rangle$ -type dislocations in the as-received Mg alloy. During high temperature ECA pressing (at 270 °C) the fraction of  $\langle c+a \rangle$ -type dislocations increases. The correlation between the microstructure and the room and high temperature mechanical behavior is also studied and discussed.

S - O11

## COMPOSITION VARIATIONS IN LINE BROADENING ANALYSIS

A. Leineweber, E. J. Mittemeijer

Max Planck Institute for Metals Research, Heisenbergstraße 3, 70569 Stuttgart, Germany

In the course of an analysis of broadened powder diffraction-line profiles the separation of different contributions to the overall physical line broadening is required. E. g. several methods exist to separate size and microstrain broadening due to their different dependencies on the reflection order.

The most prominent source of microstrain broadening are microstresses around extended defects like dislocations. Another, less frequently considered origin of microstrain broadening is local variation in composition [1] which leads to local variations in the lattice parameters. In the simplest case composition varies only between different coherently diffracting domains, i.e. each domain has its own characteristic lattice parameters which are themselves a usually monotonous function of composition. In such cases the diffraction patterns are simple superpositions of the diffraction patterns originating from the different compositions.

In general the probability density function of composition is expressed in the diffraction line profile of each reflection  $hkl$ , according to the dependence of the d-spacing  $d_{hkl}$  on composition. This compositional contribution to the line broadening can be very complicated and has to be convoluted with other occurring sources of line broadening and the instrumental resolution.

For relatively narrow and symmetrical unimodal composition distributions around an average composition the widths  $B_{hkl}$  of the reflections on the diffraction angle  $2\theta_{hkl}$  scale vary for a certain direction of the diffraction vector like

$$B_{hkl} \propto A(hkl) \tan \theta_{hkl} \quad (1)$$

with  $A(hkl)$  being an anisotropy factor which varies with the direction of the diffraction vector but not with its length (i.e. with  $2\theta_{hkl}$ ).  $A(hkl)$  can be expressed as

$$A(hkl) = d_{hkl}^2 \left| \frac{D_{HKL} h^H k^K l^L}{H K L 2} \right| \quad (2)$$

The parameters  $D_{HKL}$  can be calculated from the dependencies of the reciprocal metrical matrix components on composition and the width of the composition distribu-

*This work was supported by the Hungarian Scientific Research Fund, OTKA, Grant Nos. F-047057, T-046990 and T-042714.*

- [1] V. V. Stolyarov, Y. T. Zhu, I. V. Alexandrov, T. C. Lowe, R. Z. Valiev, *Materials Science and Engineering A* 343 (2003) 43.
- [2] T. Ungár, A. Borbély, *Appl. Phys. Lett.* 69 (1996) 3173.
- [3] T. Ungár, J. Gubicza, G. Ribárik, A. Borbély, *J. Appl. Cryst.* 34 (2001) 298.
- [4] I.C. Dragomir, T. Ungár, *J. Appl. Cryst.* 35 (2002) 556.
- [5] R. Kuzel jr., P. Klimanek, *J. Appl. Cryst.* 22 (1989) 299.

tion function. The symmetry restrictions for the dependencies of the reciprocal metrical matrix components on composition reflect the crystal system and thus impose symmetry restrictions on  $D_{HKL}$ , since the influence of the composition distribution on the line width is the same for all reflections. This leads to one parameter  $D_{HKL}$  for the cubic system (i.e. the line broadening is isotropic) and six parameters  $D_{HKL}$  for the triclinic system. For sufficiently (pseudo-)Voigt-like composition distributions anisotropic line broadening according to Eqs. 1-2 can conveniently be incorporated into a Thompson-Cox-Hastings pseudo-Voigt function profile function [2] in the course of a Rietveld refinement.

The anisotropic line broadening as given by Eq. 1-2 constitutes a *physically founded* special case of a previously proposed *phenomenological* model for anisotropic microstrain broadening [3, 4] having an anisotropy factor of

$$A(hkl) = d_{hkl}^2 \sqrt{\frac{S_{HKL} h^H k^K l^L}{H K L 4}} \quad (3)$$

which is to be combined with Eq. 1. In order that Eq. 3 is identical with Eq. 2, additional symmetry restrictions on  $S_{HKL}$  have to be introduced, only then Eq. 3 could be used to describe the anisotropic line broadening due to composition variations as well.

Different examples of diffraction line broadening from more or less inhomogeneous solid solution samples will be presented. Possibilities to distinguish compositional microstrain broadening from other types of line broadening, as well as problems encountered in such analyses will be presented.

- [1] Leineweber, A. & Mittemeijer, E.J., *J. Appl. Crystallogr.* 37 (2004) 123.
- [2] Thompson, P., Cox, D. E. & Hastings, J. B., *J. Appl. Crystallogr.* 20 (1987) 79-83.
- [3] Stephens, P.W., *J. Appl. Crystallogr.* 32 (1999) 281.
- [4] Popa, N.C., *J. Appl. Crystallogr.* 31 (1998) 176.



S - O12

## SIZE ANISOTROPY AND LOGNORMAL SIZE DISTRIBUTION IN THE POWDER DIFFRACTION WHOLE PATTERN FITTING

N. C. Popa<sup>a, b</sup> and D. Balzar<sup>c, d</sup>

<sup>a</sup>Frank Laboratory of Neutron Physics, Joint Institute for Nuclear Research, 141980 Dubna, Moscow Region, Russia; <sup>b</sup>National Institute for Materials Physics, P.O. Box MG-7, Bucharest, Romania; <sup>c</sup>Department of Physics and Astronomy, University of Denver, Denver, CO 80208, USA; <sup>d</sup>National Institute of Standards and Technology, Boulder, CO 80305, USA.

The approach developed by Popa and Balzar [1] to model the size broadening in powder diffraction patterns by samples with lognormal size distribution of spherical crystallites can be easily extended to include size anisotropy if the crystallite shape is approximated by an ellipsoid.

In comparison with the existing approaches using ellipsoids to describe the size anisotropy, this approach uses a peak breadth symmetrized according to the crystal Laue class.

The proposed model was tested on a zinc oxide diffraction pattern measured in a Bragg – Brentano geometry. The model is compared with the previously proposed model using spherical harmonics to describe the size anisotropy [2].

[1] Popa, N. C. & Balzar, D. (2002). *J. Appl. Cryst.* **35**, 338-346.

[2] Popa, N. C. (1998). *J. Appl. Cryst.* **31**, 176-180.

S - O13

## SIMPLIFIED MICROSTRUCTURAL MODELS TO ANALYZE ANISOTROPIC SIZE AND STRAIN

Juan Rodríguez-Carvajal

Laboratoire Léon Brillouin (CEA-CNRS), CEA/Saclay, 91191 Gif sur Yvette Cedex, France.

A summary of the different approaches to extract and interpret microstructural parameters from powder diffraction techniques will be presented. Special emphasis will be devoted to the so-called Voigt model for both the instrumental and the intrinsic diffraction peak shape. Under this last assumption many kinds of microstructural effects can be studied in a simplified manner. This quite general model is fully implemented and ready to be used in the computer program FULLPROF together with the Rietveld method. Complex anisotropic peak broadening may be due to size and strain effects, a complementary electron microscopy study is often needed to disentangle and evaluate the main (size or strain) contribution to broadening.

To treat anisotropic size effects it is extremely useful, in many cases, to use linear combinations of spherical harmonics to model the Lorentzian part of the peak broadening. The apparent sizes along different directions can be reconstructed from the refined coefficients and an average “apparent shape” of the coherent domains of the sample can be obtained. Some examples taken from battery positive electrode materials and catalysis will be presented, one of them is shown in Figure 1.

In case of dominant anisotropic broadening due to microstrains (high number of dislocations, vacancies, twin faults, solid solution effects, etc.) a phenomenological ap-

proach introduced 13 years ago [1] and based in the assumption that all the defects responsible of the broadening can be reduced to fluctuations and correlations of cell parameters, or any combination of them, has proven to be extremely useful. A convenient formulation derived from [1] when the metric parameters are the coefficients of the quadratic form in  $(hkl)$  constituting the square of a reciprocal lattice vector was proposed by Stephens [2] and a similar one, based in elasticity theory, was previously proposed by Popa [3]. We will show that there are many equivalent ways to treat anisotropic strain broadening, using the assumptions first published in [1], that can help to construct physical models for the origin of the anisotropic microstrain broadening. Some examples taken from different kind of materials (intermetallics, oxides) in different contexts (phase transitions, reducing synthesis conditions, etc.) will be presented.

[1] J. Rodríguez-Carvajal, M. T. Fernández-Díaz, J. L. Martínez, *J. Phys. Cond. Matter* **3**, 3215 (1991).

[2] P. W. Stephens, *J. Appl. Cryst.* **32**, 281 (1999).

[3] N. C. Popa, *J. Appl. Cryst.* **31**, 176 (1998).

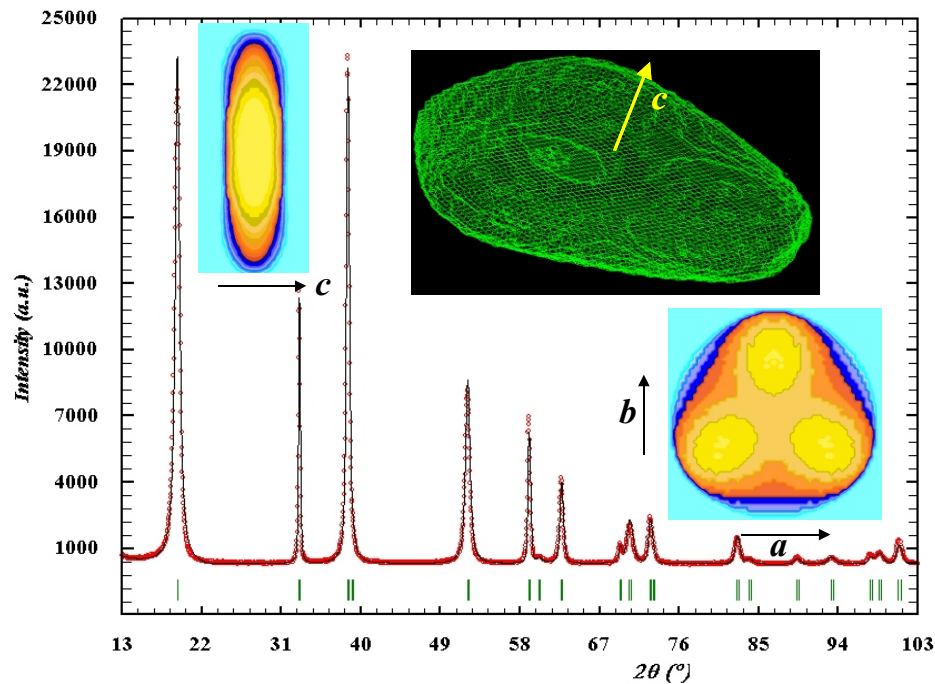


**Figure 1:** Example of conventional X-ray (Cu-K $\alpha$ ) Rietveld refinement of a Ni(OH) $_2$  sample ( $P-3m1$ ,  $a = 3.13 \text{ \AA}$ ,  $c = 4.61 \text{ \AA}$ ), with a strong anisotropic peak broadening, using spherical harmonics for size effects. The insets show the “average apparent shape” of the crystallite coherence domains in different directions.

S - O14

## EVALUATION OF SIZE AND STRAIN PARAMETERS FROM X-RAY PEAKS BY THE MOMENTUM METHOD

A. Borbély, Á. Révész, I. Groma

*Eötvös University, Department of General Physics, H-1518, POB. 32, Budapest, Hungary.*

Determination of meaningful and reliable size and strain parameters from X-ray peaks is a challenging task for nowadays evaluation techniques. In this respect microstructurally based models are welcome since they predict the shape of X-ray peaks, which can be directly compared with experiment. This is especially true for nanomaterials when due to the small particle size a nearly Lorentzian peak shape is expected. If the particles contain lattice defects, then the resulting profile is given the convolution of the transform of the size profile and the transform of the profile characteristic for the relevant lattice defect. It is known that in case of dislocations (the most frequently encountered lattice defect) the tail of the profile varies as  $q^{-3}$ , where  $q$  is the deviation from the reciprocal lattice point. According to the general theory of dislocation induced X-ray peak broadening [1,2] only this asymptotic behaviour can be anticipated, the shape of the whole profile being unknown. Exception from this is the special case of restrictedly random distribution of dislocations, a model developed by Wilkens, who has calculated the entire peak shape [3]. It is however, questionable if this special dislocation distribution is valid in any practical situation. If not, it is safer to consider only the asymptotic behaviour of the X-ray peaks. This doesn't mean however, that the Wilkens model and its incorporation in multi-profile fitting programs [4], to replace less physically justified peak-func-

tions, is not applicable. We only want to stress that in such cases a microstructural justification of the selected evaluation method should be given. If the selected method cannot be justified, then only the general model is reliable.

Since a general peak-function applicable to each investigated case has not been found yet, we will discuss the asymptotic method. The kinematic theory of X-ray scattering predicts at large  $q$  values a  $q^{-2}$  and  $q^{-3}$  dependence of the scattered intensity, for the cases of small crystallite size [5] and dislocation [2] produced broadening, respectively. Commonly the measurements contain statistical errors, which may be reduced if an integral evaluation method is selected. Extending the variance method of Wilson [5], the authors have proposed recently a momentum method for the evaluation of the average particle size and dislocation density [6], when both sources of broadening are present. According to the  $q$  dependencies mentioned above the different order moments of the scattered intensity have typical behaviours. For example the fourth order moment divided by  $q^2$  is constant when broadening is produced by dislocations and shows linear  $q$  dependence for particle type broadening. The great advantage of the momentum method is that one can readily see the type of broadening present in the experiment and verify if the assumptions of small particle size or presence of dislocations applies. The method is exemplified on measurements done on ball-milled and



heat-treated aluminium powder samples. An error analysis of the evaluated parameters is presented also.

#### Acknowledgement

The authors acknowledge the financial support of the Hungarian Research Found OTKA under the contracts no. T034999 and T043519.

- [1] Groma, I., Ungár, T., Wilkens, M. *J. Appl. Cryst.* 21 (1988) 47.  
 [2] Groma, I. *Phys. Rev. B* 57 (1998) 7535.

- [3] Wilkens, M. *Fundamental Aspects of Dislocation Theory*, National Bureau of Standards (US) Special Publication No. 317, Vol. II, edited by J. A. Simmons, R. de Wit & R. Bullough, (1970) pp. 1195-1221. Washington, DC: N.B.S.  
 [4] Ungár, T., Gubicza, J., Ribarik, G. and A. Borbély, J. *Appl. Cryst.*, 34 (2001) 298.  
 [5] A. J.C. Wilson, *Proc. Phys. Soc.* 80 (1962) 286; *ibid.* 81 (1963) 41.  
 [6] Borbély, A. és Groma, I. *Applied Physics Letters*, 79 (2001) 1772.

S - O15

## X-RAY DIFFRACTION FROM EPITAXIAL THIN FILMS : AN ANALYTICAL EXPRESSION OF THE LINE PROFILES ACCOUNTING FOR MICROSTRUCTURE

A. Boulle, R. Guinebretiere, A. Dauger

*Science des Procédés Céramiques et de Traitements de Surface – CNRS UMR 6638, ENSCI, 47 r 73 avenue Albert Thomas 87065 Limoges Cedex*

The effect of finite crystal size on the X-ray diffraction line profiles is known since the experiment of Friedrich, Knipping and Laue [1] who first derived the formula known as the Laue function :  $\sin(Qt/2)/\sin(Qd/2)$ , where  $Q$ ,  $t$  and  $d$  are the length of the scattering vector, the crystal thickness and the interplanar spacing in the direction of the scattering vector. Since that time a large amount of work has been devoted to the extraction of information concerning 'size' and 'strain' from the XRD line profiles [2,3], with particular emphasis being laid on polycrystalline materials. In such systems the kinematical theory of diffraction was shown to apply very well. Concerning epitaxial thin films, the high crystalline quality layers that are achievable using molecular beam epitaxy or chemical vapor deposition strongly promoted the use of the more rigorous dynamical theory of diffraction [4]. Up to recently these studies mainly focused on semiconductor materials.

In the recent years much attention has been paid on oxide epitaxial thin films, but real structure effects (e.g. random lattice spacing fluctuations, thickness fluctuations, roughness...) remain difficult to incorporate into the dynamical scattering theory. Moreover, the relative imperfection of oxide thin films (as compared to semiconductors) enables to use the kinematical theory. However, the presence of defects strongly alters the shape of the intensity distribution predicted by Laue. Several authors modified this expression in order to account for the effect of one of the above-mentioned defect [5,6], but up to now the combined effects of different defects are in general handled using a numerical integration of the expression of the intensity distribution.

In this communication we derive an analytical interference function able to describe the XRD line profiles of an epitaxial thin film with a microstructure made of different type of defects: film thickness fluctuation, roughness, cumulative and non-cumulative random lattice spacing fluctuations. The derivation is carried-out within the framework of the kinematical scattering theory. For brev-

ity, in this abstract we focus on the coherently scattered intensity,  $I = \langle E \rangle \langle E^* \rangle$ . The effect of diffuse scattering will be discussed at the conference. The scattered amplitude distribution,  $\langle E \rangle$ , of a thin film with a rough interface and a fluctuating thickness can be written [7]:

$$\langle E(q_z) \rangle = F_h \int_0^t dz_1 dz_2 p(t) p(z_1) \exp(iq_z z_1)$$

$q_z$  is the z-component of the reduced scattering vector  $\mathbf{q} = \mathbf{Q} - \mathbf{h}$ ,  $\mathbf{h}$  being the reciprocal lattice vector of the reflection (the z axis is chosen parallel to the outwards film surface normal).  $t$ ,  $z_1$  and  $F_h$  are the film thickness, the coordinate of the interface, the film shape factor (1 inside, 0 outside the film) and the structure factor, respectively.  $p(x)$  is the probability density function of the variable  $x$ . It can further be shown that cumulative random lattice spacing fluctuations can be accounted for by making the substitution:

$$q_z \rightarrow q_z + i \frac{Q^2 \langle u^2 \rangle}{2d}$$

where  $\langle u^2 \rangle$  is the root mean squared (rms) cumulative lattice displacement. Making the assumption that all  $p(x)$  are given by normal distributions it turns out that:

$$I(Q) = \frac{|F_h|^2}{q_z^2 \frac{Q^2 \langle u^2 \rangle}{2d}} \exp(-Q^2 \langle u^2 \rangle \frac{t^2}{d})$$

$$1 - \exp(-Q^2 \langle u^2 \rangle \frac{t}{d})$$

$$2 \exp(-Q^2 \langle u^2 \rangle \frac{t}{d}) \cos(q_z \langle t \rangle)$$

with

$$\frac{2}{l} \frac{2}{l} \frac{2}{s} 2r \frac{1}{l} \frac{1}{s}$$

where  $\langle u^2 \rangle$ ,  $l$ ,  $s$ , and  $r$  are the rms lattice displacements, the rms interface roughness, the rms surface roughness and

interface-surface roughness correlation coefficient ( $r = 1$  correlated,  $r = 0$  uncorrelated,  $r = -1$  anti-correlated). The effects of these microstructural parameters (computed with the above equation) are shown in fig.1 and fig. 2. and will be further discussed at the conference together with the assumptions made.

- [1] W. Friedrich, P. Knipping, M. Laue, *Annalen der Physik* 14, 971-990, 1913.  
 [2] R. L. Snyder, J. Fiala, H. J. Bunge (Eds), *Defect and microstructure analysis by diffraction*, IUCr Monographs on crystallography 10 (Oxford University Press Inc, New-York) 1999.

- [3] E. J. Mittemeijer, P. Scardi (Eds), *Diffraction analysis of the microstructure of materials*, Springer series in materials science (Springer-Verlag, Berlin Heidelberg) 2004.  
 [4] A. Authier, *Dynamical theory of X-ray diffraction*, IUCr monographs on crystallography 11. (Oxford University Press, New-York) 2001.  
 [5] P. F. Miceli, C. J. Palmstrom, K. W. Moyers, *Appl. Phys. Lett.* 61 17, 2060-2062, 1992.  
 [6] E. Zolotoyabko, *J. Appl. Cryst.* 31, 241-251, 1998.  
 [7] A. Boulle, R. Guinebreti re, A. Dager, *J. Phys. IV France* (2004) to be published.

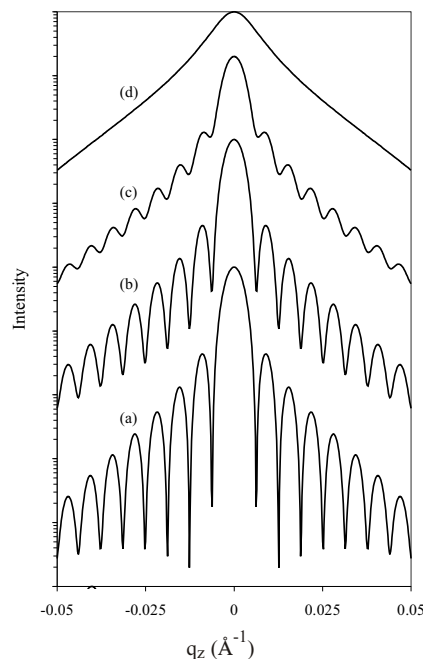
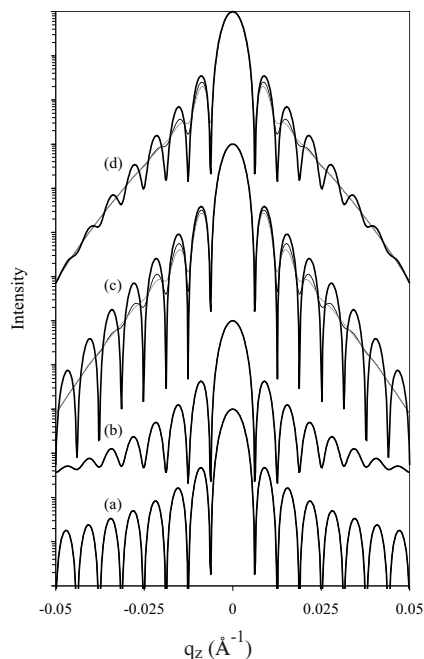


**Fig.1** (left) : effect of  $\sigma_1$  and  $\sigma_s$  on the line profile of 100nm-thick film. (a)  $\sigma_1 = \sigma_s = 0$ ; (b)  $\sigma_1 = 0$ ,  $\sigma_s = 5$  nm ; (c)  $\sigma_1 = 5$  nm,  $\sigma_s = 5$  nm ; (d)  $\sigma_1 = 5$  nm,  $\sigma_s = 10$  nm ( $r = 1$  bold black line,  $r = 0$  black line,  $r = -1$  gray line).

**Fig.2** (right): effect of cumulative lattice spacing fluctuations. (a)  $\sigma_u^{(c)} = 0$  ; (b)  $\sigma_u^{(c)} = 0.05$  Å ; (c)  $\sigma_u^{(c)} = 0.1$  Å ; (d)  $\sigma_u^{(c)} = 0.2$  Å.

